THE JOURNAL OF PHYSICAL CHEMISTRY A

Article

pubs.acs.org/JPCA

Wetting Transitions of Water on Graphite and Graphene

Hye-Young Kim,*[,†] Maria Cristina dos Santos,[‡,§] and Milton W. Cole[§]

[†]Department of Chemistry and Physics, Southeastern Louisiana University, Hammond, Louisiana 70402, United States

[‡]Instituto de Física, Universidade de São Paulo, 05508-090 São Paulo, SP, Brazil

[§]Department of Physics, Penn State University, 104 Davey Lab, University Park, Pennsylvania 16802, United States

ABSTRACT: Water has been predicted theoretically and observed experimentally to exhibit a wetting transition on graphite. Previous study of this problem was based on quite uncertain water−graphite interaction potentials. This paper computes the wetting temperature on graphite using recent, more realistic, interactions. Similar calculations are presented for the case of water on a suspended (free-standing) graphene sheet.

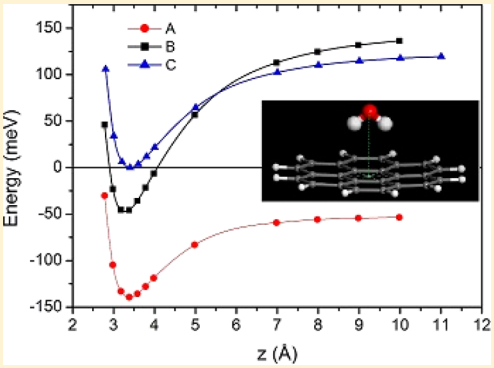

1. INTRODUCTION

One of the most remarkable phenomena associated with fluids on solid surfaces is the *wetting transition*. As first predicted in the 1970s, this transition is observed under saturated conditions at a temperature T_w, the wetting temperature, at which the contact angle of a liquid drop falls to zero.[1−4] This point, at saturated vapor pressure, P_{svp}, is one terminus of a first-order transition line $P_{transition}(T)$ in the $P-T$ plane; at the other end of this line is a prewetting critical point, at pressure $P = P_{transition}(T_{pwcp})$. At intermediate points, this line is observed in adsorption isotherm experiments as a discontinuous jump in film coverage as a function of pressure. The wetting transition is described by the 2D Ising model, an analogue of the 3D liquid↔vapor transition. The order parameter is the film's areal density, a function $\rho(x,y)$ of the $x-y$ coordinates along the surface.

Until recently, evidence concerning these transitions was limited to two very different kinds of system. The most common examples of the phenomenon involve inert gases and hydrogen on various alkali metal surfaces at cryogenic temperatures. A very different regime is that seen for mercury on sapphire at very high temperature ($T_w \approx 1600$ K).[5] Nearly a decade ago, Gatica et al.[6] predicted that a similar wetting transition should occur for water on graphite and other surfaces at an *intermediate* temperature. Their prediction of T_w depended, however, on a very uncertain parameter, the well depth D of the water adsorption potential. If $D = 25$ kJ/mol (~250 meV), for example, then the predicted $T_w \approx 340$ K, while if $D \approx 10$ kJ/mol, then $T_w \approx 500$ K. These predictions rely on the so-called "simple model" (SM) of the wetting transition, which has been remarkably successful in predicting wetting temperatures[4] for inert gas fluids. In the specific case of water/graphite, Zhao's simulations[7] found that the model's prediction was accurate; using the Zhao−Johnson potential[8] ($D \approx 9.7$ kJ/mol), the SM predicts $T_w = 474$ K, while the simulation results found 475 K < T_w < 480 K.

Quite recently, experiments of Friedman, Khalil, and Taborek[9] have confirmed this theoretical expectation of water-wetting transitions within this intermediate temperature regime. They reported transition temperatures $T_w = 458$, 507, and 544 K, on quartz, sapphire, and graphite, respectively. These results have motivated the present study of water wetting on graphite and suspended graphene. Here we address a set of recent ab initio potentials for water[10−15] on these surfaces and their implications for the wetting transition. In future work, we will address the similar behavior of water on the other surfaces studied experimentally.

In the following section, we summarize the various results obtained recently for D of water on graphene and graphite. Using these, we employ the "simple model" to estimate the wetting temperatures on these surfaces. This model, as used by Gatica et al.,[6] provides an explicit relationship between the adsorption potential well depth and the coefficient C_3 of the water-graphite z^{-3} van der Waals interaction

$$(C_3 D^2)^{1/3} = 3.33\left(\frac{\sigma_{lg}}{\rho - \rho_v}\right)_{T_w} \approx 3.33\left(\frac{\sigma_{lg}}{\rho}\right)_{T_w}$$

Here σ_{lg} is the liquid−gas interfacial tension and ρ and ρ_v are the liquid and vapor density, respectively, all at the wetting temperature. The last step is taken because $\rho \gg \rho_v$ except near

Special Issue: A. W. Castleman, Jr. Festschrift

Received: January 29, 2014
Revised: March 4, 2014
Published: March 11, 2014

   dx.doi.org/10.1021/jp501046r | J. Phys. Chem. A 2014, 118, 8237−8241

T_c. We use this relation to compute the wetting temperature for both surfaces.

2. ADSORPTION POTENTIALS ON GRAPHENE AND GRAPHITE

In the original treatment of Gatica et al.,[6] the values of the water/graphite well-depth D_∞ were assumed to fall within the interval 9.7 to 25 kJ/mol (~100 to 260 meV) based on prior quantum chemical calculations. More recent values of D_∞ have been concentrated near the lower end of this range. An ab initio calculation of Ma et al.[10] resulted in values near D_{mono} = 8.1 kJ/mol (84 meV) for two-leg and 6.8 kJ/mol (71 meV) for one-leg for two orientations of water molecules on graphene, with ~15% uncertainty depending on the computational method used.[11,12] (These molecular configurations are discussed later.) A number of quantum-chemical calculations have been carried out for a water molecule on a series of aromatic hydrocarbons, culminating in coronene, from which it was possible to extrapolate to yield a value on graphene. The resulting values include a range from 10 to 16 kJ/mol (104 to 165 meV). While this range of uncertainty is somewhat narrower than that of the previous study, it remains unfortunately large, precluding a very precise prediction of the wetting temperature. These calculations are described briefly in the Discussion Section later.

We now address the question of the relationship between the adsorption potential on graphene and that on graphite. We consider the latter to consist of a top graphene layer (j = 1) and subsequent layers j = 2, 3, ... ∞. (See Figure 1.) Suppose that

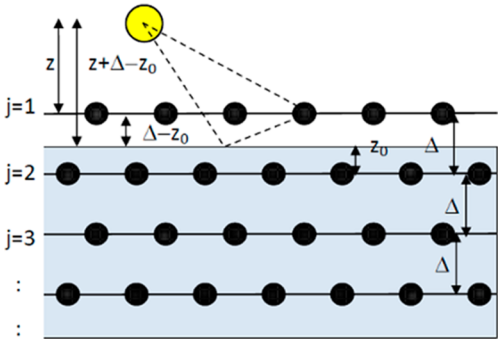

Figure 1. Schematic description of the water on graphite system. The large filled circle represents the water molecule, while the smaller dark circles represent C atoms. The shaded region represents the continuum substrate.

the water molecule is located a distance z above the graphene plane. We may write $V_\infty(z)$, the molecular potential on graphite, in terms of the potential on graphene, $V_{mono}(z)$, plus contributions from all of the other layers, plus a term denoted $\Delta V_3(z)$, a three-body correction to the additive approximation:

$$V_\infty(z) = V_{mono}(z) + \sum_{j=2} V_{mono}(z + jD) + \Delta V_3(z) \quad (1)$$

$$V_\infty(z) \approx V_{mono}(z) + V_\infty(z + \Delta - z_0) + \Delta V_3(z) \quad (2)$$

Here Δ = 3.35 Å is the interlayer spacing of graphite and the second term $V_\infty(z + \Delta - z_0)$ represents the continuum version of the sum in eq 1 over graphite layers, n = 2 to ∞, where the continuum is terminated midway between the top two planes (as justified by the Euler−Maclaurin summation formula). This equation is exact, apart from the continuum approximation. Within the same approximation, we may evaluate $\Delta V_3(z)$ from the McLachlan theory[16] of many-body interactions at surfaces, applied to the geometry depicted in Figure 1

$$\Delta V_3(z) = \sum_{\mathbf{R}} V_{McLachlan}(z, \mathbf{R}) \quad (3)$$

Here we indicate schematically a sum over all of the atoms of the graphene sheet (all **R**) of the McLachlan three-body interaction between a carbon atom in the graphene, the water molecule, and the graphite continuum below (j = 2 to ∞).

First, in the framework of first-order perturbation theory, by neglecting the McLachlan term $\Delta V_3(z)$, the well depth of the holding potential of a water molecule on a graphite surface (D_∞) can be written as a sum of the well depth (D_{mono}) of the holding potential of a water molecule on a graphene sheet and the van der Waals interaction of the water molecule with the graphite continuum below

$$D_\infty = D_{mono} + C_3/(z_{min} + \Delta - z_0)^3 \quad (4)$$

Here z_{min} is the height of the adsorbed water molecule above the graphene sheet. In the present case, the water molecule is far from the graphite subsurface layers (j = 2 to ∞). Therefore, it is reasonable to assume that the contribution of the repulsive part of the potentials to the total well depth (D_∞) is purely due to the graphene sheet (j = 1). Hence, the repulsive part of $V_\infty(z + \Delta - z_0)$ is neglected. The second term in eq 4 is the van der Waals dispersion interaction of the water molecule adsorbed on a continuum graphite, and C_3 = 1075 meV-Å^3, derived by Gatica et al.[6] As an example, using the values of the continuum image plane position previously shown ($z_0 = \Delta/2$) and an adsorption height z_{min} = 3.5 Å, we explicitly calculate the "correction" term

$$C_3/(z_{min} + \Delta/2)^3 \approx 1075\ \text{meV·Å}^3/(3.5\ \text{Å} + 3.4\ \text{Å}/2)^3 = 7.65\ \text{meV} \quad (5)$$

Hence, in this first approximation, the well depth on graphite is just ~10% greater than that on graphene, so we conclude that the net well depth on graphite is D_∞ ~93 ± 10 meV. This conclusion leads to a wetting temperature somewhat >510 K. Note that the small value of this energy justifies the perturbation theory a posteriori.

Now, let us evaluate the higher order theory, including the McLachlan energy. Following the procedure outlined in ref 17, the McLachlan substrate-mediated interaction of a water molecule and carbon atoms on graphene, after making a continuum integration over the carbon atoms in the graphene, is

$$\Delta V_3 = -(\pi C_{s2}/2A)/[z_{min} + 2(\Delta - z_0)]^4 \quad (6)$$

Here A (= 2.62 Å^2) is the area per carbon atom on graphene. There are two coefficients that must be calculated

$$C_{s2} = (g_0 C_{s1}/2)(2 + y_C + y_W + y_C/(1 + y_W) + y_W/(1 + y_C))/(1 + y_C + y_W) \quad (7)$$

$$C_{s1} = (3g_0\alpha_{0C}\alpha_{0W}E_S y_C y_W/2)(1 + y_C + y_W)/\{(1 + y_C)(1 + y_W)(y_C + y_W)\} \quad (8)$$

Here the subscripts C, W, and S refer to the carbon atoms in the "adlayer" graphene (j = 1), the water molecule, and the substrate (graphite continuum from j = 2 to ∞). We treat water molecule as an atom (i.e., an isotropic molecule) for this

dx.doi.org/10.1021/jp501046r | J. Phys. Chem. A 2014, 118, 8237−8241

Table 1. Graphite Well-Depth Calculations, Based on Alternative Assumed Values, Derived from (Graphene Well Depth) D_{mono} = 84 meV for the Two-Leg Configuration and One-Leg Configuration, with D_{mono} = 71 meV[a]

					two-leg		one-leg	
z_{min} (Å)	Δ(Å)	z_0 (Å)	ΔV_3 (meV)	$C_3/[z + (\Delta - z_0)]^3$ (meV)	D_{mono} (meV)	D_∞ (meV)	D_{mono} (meV)	D_∞ (meV)
3.5	3.4	1.7	−1.31	7.65	84	90.34	71	77.34
	3.35	1.675	−1.34	7.76		90.41		77.41
	3.4	1.0	−0.62	5.23		88.61		75.61
	3.35	1.0	−0.65	5.37		88.71		75.71
3.6	3.4	1.7	−1.23	7.22		89.99		76.99
	3.35	1.675	−1.27	7.32		90.05		77.05
	3.4	1.0	−0.59	4.98		88.38		75.38
	3.35	1.0	−0.62	5.10		88.48		75.48
3.83*	3.4	1.7	−1.08	6.36		89.27		76.27
3.805*	3.35	1.675	−1.13	6.53		89.40		76.40
3.13*	3.4	1.0	−0.75	6.36		89.61		76.61
3.13*	3.35	1.0	−0.79	6.53		89.74		76.74

[a]These D_{mono} are the averages of results of DMC and RPA methods.[10]

simple model calculation because there exists no McLachlan-type analytic equation for the case of an anisotropic molecule. Conventional values for the atomic parameters are adopted: g_0 = 0.619, α_{0C} = 1.1 Å^3, α_{0W} = 1.43 Å^3, E_S = 18.1 eV, E_W = 17.7 eV, and E_C = 16.2 eV, from which we obtain $y_C \equiv E_C/E_S$ = 0.895, $y_W \equiv E_W/E_S$ = 0.978, C_{s1} = 9469 meV·Å^6, and C_{s2} = 4939 meV·Å^6.

It should be noted how sensitive ΔV_3 and D_∞ are to the position z of the water molecule, whose value differs in calculations by various workers. We therefore present in Table 1 results calculated with various assumed values of z_{min}, Δ, z_0, and D_{mono} for two-leg and one-leg configurations (depicted schematically in Figure 2). Two commonly adopted values of

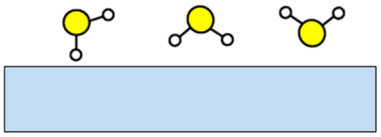

Figure 2. Schematic depiction is the orientation of water molecules on graphite or graphene. From left to right, one-leg, two-leg, and inverted two-leg configurations.

the interlayer spacing in graphite (Δ) are 3.4 and 3.35 Å. Two alternative values of the image plane position are z_0 = Δ/2 and 1.0 Å.[18,19] The z_{min} values noted with an asterisk in the last four rows in the Table 1 are estimated from the experimentally fitted value of $(C_3 D_\infty^2)^{1/3}$ = 180 meV·Å[9] and the relation $(z_{min} - z_0) = (2C_3/3D_\infty)^{1/3}$ for water on graphite. We note here that from fitting the experimental data to continuum adsorption potential the well-depth D_∞ estimated is 73.7 meV using C_3 = 1075 meV·Å^3.

Even with uncertain values of parameters used in the calculations in Table 1, the standard deviation is small, <1 meV, which is ∼1% of the average values, D_∞ = 89 and 76 meV for two-leg and one-leg configurations, respectively. On the basis of the simple model (figure 1 of ref 6), these well-depth values predict the wetting transition temperatures for two-leg and one-leg configurations on graphite to be 515 and 522 K, respectively.

We recall that the experimentally measured wetting temperature on graphite is T_w = 544 ± 12 K,[9] and our estimated well depth and adsorption height are, respectively, around 73.7 meV and 3.8 to 3.1 Å, depending on which value is used for the continuum boundary cutoff parameter z_0. This estimate was made using the first-order approximation previously mentioned. The well-depth values listed in Table 1 suggest that the one-leg configuration is less energetically favored than the two-leg configuration on graphite. However, one should bear in mind that the correlation effects ignored by the simple model may be particularly significant for water (compared with the inert gases). As the film density increases to a monolayer or beyond, the hydrogen-bonding interaction might lead the individual water molecules to assume one-leg (or even inverted-two-leg) configurations, even though that is less favored for a single molecule.[20] We note here that in this range of temperature (∼500 K) the water molecules are expected to rotate freely. Therefore, the thermally averaged values of adsorption height and wetting temperature are appropriate. More generally, one must recognize that only finite temperature simulations can resolve this problem.

The well depth of the potential on a graphene is smaller than that on a graphite basal plane, that is, 84 and 71 meV for two-leg and one-leg configurations,[10] respectively. The corresponding wetting temperatures predicted by the simple model are 520 and 534 K for two-leg and one-leg configurations, respectively, on graphene. (Again, the thermally averaged value of these wetting temperatures is expected at this high temperature.) Additionally, when a wetting experiment is performed on a free-standing graphene, the binding energy of a water film should include the interaction between the adsorbed water molecules on opposite sides of the graphene. While this film−film interaction was found to be small for inert gas wetting transitions,[19] it may be of greater relative importance for water.

As a last remark on the simple model, we would like to address the question on how the correction due to the three-body dipole interaction compares with that due to the water-dipole/graphene-quadrupole interaction, which has not been considered in this work. A number of studies incorporating the quadrupole of graphite have employed conflicting signs of the C quadrupole. To the best of our knowledge, this controversy has not been resolved. In any case, the water-dipole/graphene-quadrupole interaction was found to be small if not to vanish

dx.doi.org/10.1021/jp501046r | J. Phys. Chem. A 2014, 118, 8237−8241

exactly,[14,21] and thus the dipole/quadrupole interaction is not included in our calculation.

3. SUMMARY AND DISCUSSION

New calculations have been carried out to predict the wetting temperature of water on graphite and free-standing graphene. Using new ab initio adsorption potentials for water/graphene and explicit calculations of van der Waals corrections, the simple model yields results that come close to the recently measured wetting temperatures for water on graphite. There remains some uncertainty in these predictions that is a consequence of uncertainty in the potentials themselves. In the case of a free-standing graphene surface, the adsorption potential is some 10% less attractive than for graphite, implying a wetting temperature about 20 K higher on the graphene sheet than on graphite.

We would like to address aspects of the "background" problem of an uncertain potential. Quantum-chemical and other many-body calculations of water adsorption are currently subjects of intensive research. A distinction can be made between wave-function-based methods (WFT) and density-functional-theory methods (DFT).[22] WFT methods (e.g., the coupled-cluster method, including single and double excitations plus perturbative triple excitations, CCSD(T)) yield accurate benchmark results, but they are restricted to systems comprising a few tens of atoms. In contrast, DFT methods are computationally efficient, but the conventional functionals accounting for exchange-correlation interactions do not describe dispersion. This deficiency has been partially corrected by the inclusion of an explicit (semiempirical) $-C/R^6$ term in the total energy, with damping, giving rise to the so-called DFT-D methods, or by perturbation theory in the scheme called symmetry-adapted perturbation theory (SAPT).

The adsorption of water on polycyclic aromatic hydrocarbons (PAHs) has been studied within high-level correlated methods.[12] Unfortunately, the extrapolation of binding energies of increasing PAH size to obtain the energy of water on graphene is problematic because these PAHs have C−H bonds at the edges with a dipolar charge distribution due to the different electronegativities of C and H atoms. To quantify this effect, we performed calculations based on empirical potentials where we can separate effects coming from electrostatics from those related to dispersion. We used the polymer-consistent force field (PCFF),[23] as implemented in Materials Studio package[24] to model water adsorption on coronene ($C_{24}H_{12}$) and on graphene.

The PCFF energy expression contains contributions from valence terms and nonbonded interactions. These nonbonded terms, which comprise the van der Waals and electrostatic interactions, are written as sums of potential energies between pairs of atoms that are separated by at least two atoms or that belong to different molecules. The van der Waals terms are written as 6−9 Lennard-Jones potentials and a sixth power rule to obtain parameters when dealing with the interaction of a pair of atoms of different chemical elements. We assumed the C_{2v} symmetry in which the water oxygen is above the central coronene ring and the H atoms point toward opposing carbons on the central ring. In Figure 3, z is the distance of oxygen from the center of the coronene molecule. We considered three types of charge distribution: (A) all point charges are set to zero; (B) H atoms have partial charges q_H = 0.127e (e = electron charge) and the connecting C atoms have charges q_C = −0.127e, while all other atoms have partial charges set to zero;

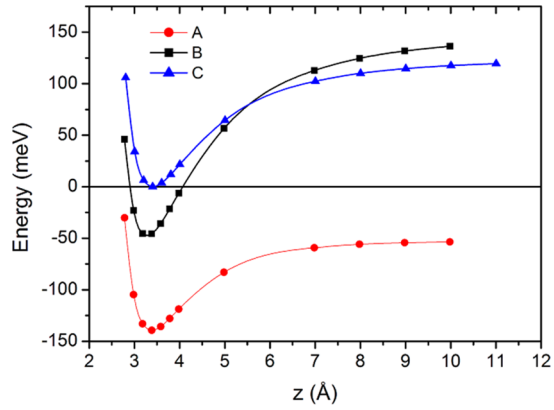

Figure 3. Total energies (millielectronvolts) as a function of the distance of oxygen from the center of coronene molecule (z) for the models A−C, as obtained from PCFF force field. The asymptotic value for each curve is an insignificant constant.

and (C) a charge distribution is calculated using the charge equilibration scheme of Rappé and Goddard,[25] which gives partial charges of q_H = 0.104e, q_{C1} = −0.130e, q_{C2} = 0.035e, and q_{C3} = 0.018e, where C1's are the carbons on C−H bonds, C2's are connected to C1's, and C3's are connected to C2's. The minimum energy of model C was used as reference.

The total energy curves are displayed in Figure 3. Note that models B and C include the electrostatic interaction among all point charges and the asymptotic behavior of the curves reflects the differences among the models. From these curves, we deduce well depths and equilibrium distances of $D_A \approx 86$ meV and z_A = 3.38 Å, $D_B \approx 190$ meV and z_B = 3.38 Å, and $D_C \approx 125$ meV and z_C = 3.40 Å. A similar procedure, now applied to a supercell representing a 10 × 10 graphene with the water molecule at the center in the C_{2v} symmetry, resulted in $D \approx 101$ meV and z = 3.40 Å. The values obtained for the model C are in very good agreement with recent quantum chemical calculations.[11,12] We thus conclude that the electrostatic interaction contributes of order 40 meV to the binding energy (the difference between models A and C). This large magnitude precludes the use of coronene as a model for graphene, where these partial charges are absent.

AUTHOR INFORMATION

Corresponding Author

*E-mail: hye-young.kim@selu.edu. Phone: 985-549-5972.

Notes

The authors declare no competing financial interest.

ACKNOWLEDGMENTS

This work has benefited from many discussions with Silvina Gatica. We are grateful to Peter Taborek for several discussions of his group's wetting data and to Mauricio Terrones for providing computational facilities, support, and helpful discussions. H.-Y.K. acknowledges support from Louisiana Board of Regents-RCS grant (LEQSF(2012-15)-RD-A-19). M.C.d.S. thanks FAPESP for financial support and the Research Computing and Cyber-Infrastructure Unit of Information Technology Services at Penn State University for providing access to the advanced computational facilities and services. M.W.C. acknowledges support from Honda Research Foundation, USA, Inc.

REFERENCES

(1) Cahn, J. W. Critical Wetting. *J. Chem. Phys.* **1977**, *66*, 3667−3672.
(2) Bonn, D.; Ross, D. Wetting Transitions. *Rep. Prog. Phys.* **2001**, *64*, 1085−1163.
(3) Saam, W. F. Wetting, Capillary Condensation and More. *J. Low Temp. Phys.* **2009**, *157*, 77−100.
(4) Gatica, S. M.; Cole, M. W. To Wet or Not To Wet. *J. Low Temp. Phys.* **2009**, *157*, 111−136.
(5) Hensel, F.; Yao, M. Wetting Phenomena Near the Bulk Critical Point of Fluid Mercury. *Ber. Bunsenges. Phys. Chem.* **1998**, *102*, 1798−1802.
(6) Gatica, S. M.; Zhao, X.; Johnson, J. K.; Cole, M. W. Wetting Transition of Water on Graphite and Other Surfaces. *J. Phys. Chem. B* **2004**, *108*, 11704−11708.
(7) Zhao, X. C. Wetting Transition of Water on Graphite: Monte Carlo Simulations. *Phys. Rev. B* **2007**, *76*, 041402.
(8) Zhao, X. C.; Johnson, J. K. An Effective Potential for Adsorption of Polar Molecules on Graphite. *Mol. Simul.* **2005**, *31*, 1−10.
(9) Friedman, S. R.; Khalil, M.; Taborek, P. Wetting Transition in Water. *Phys. Rev. Lett.* **2013**, *111*, 226101.
(10) Ma, J.; Michaelides, A.; Alfè, D.; Schimka, L.; Kresse, G.; Wang, E. Adsorption and Diffusion of Water on Graphene from First Principles. *Phys. Rev. B* **2011**, *84*, 033402.
(11) Jenness, G. R.; Jordan, K. D. DF-DFT-SAPT Investigation of the Interaction of a Water Molecule to Coronene and Dodecabenzocoronene: Implications for the Water−Graphite Interaction. *J. Phys. Chem. C* **2009**, *113*, 10242−10248.
(12) Jenness, G. R.; Karalti, O.; Jordan, K. D. Benchmark Calculations of Water−Acene Interaction Energies: Extrapolation to the Water−Graphene Limit and Assessment of Dispersion−Corrected DFT Methods. *Phys. Chem. Chem. Phys.* **2010**, *12*, 6375−6381.
(13) Cabaleiro-Lago, E. M.; Carrazana-Garcia, J. A.; Rodriguez-Otero, J. Study of the Interaction Between Water and Hydrogen Sulfide with Polycyclic Aromatic Hydrocarbons. *J. Chem. Phys.* **2009**, *130*, 234307.
(14) Huff, E. M.; Pulay, P. A Potential Surface for the Interaction Between Water and Coronene as a Model for a Hydrophobic Surface. *Mol. Phys.* **2009**, *107*, 1197−1207.
(15) Rubes, M.; Kysilka, J.; Nachtigall, P.; Bludsky, O. DFT/CC Investigation of Physical Adsorption on a Graphite (0001) Surface. *Phys. Chem. Chem. Phys.* **2010**, *12*, 6438−6444.
(16) McLachlan, A. D. Van der Waals Forces Between an Atom and a Surface. *Mol. Phys.* **1964**, *7*, 381−388.
(17) Klein, J. R.; Bruch, L. W.; Cole, M. W. Many Body Interactions in Physisorption: Nonadditivity of Film and Substrate Contributions to the Holding Potential. *Surf. Sci.* **1986**, *173*, 555−564.
(18) Kim, H.-Y.; Cole, M. W. Substrate Mediation of the Interaction Between Adatoms on Graphite: Discrete Lattice Model. *Surf. Sci.* **1988**, *194*, 257−264.
(19) Bruch, L. W.; Cole, M. W.; Kim, H.-Y. Transitions of Gases Physisorbed on Graphene. *J. Phys.:Condens. Matter* **2010**, *22*, 304001.
(20) Rubes, M.; Nachtigall, P.; Vondrasek, J.; Bludsky, O. Structure and Stability of the Water-Graphite Complexes. *J. Phys. Chem. C* **2009**, *113*, 8412−8419.
(21) Kocman, M.; Pykal, M.; Jurečka, P. Electric Quadrupole Moment of Graphene and its Effect on Intermolecular Interactions. *Phys. Chem. Chem. Phys.* **2014**, *16*, 3144−3152.
(22) Riley, K. E.; Pitonák, M.; Jurečka, P.; Hobza, P. Stabilization and Structure Calculations for Noncovalent Interactions in Extended Molecular Systems Based on Wave Function and Density Functional Theories. *Chem. Rev.* **2010**, *110*, 5023−5063.
(23) Sun, H.; Mumby, S. J.; Maple, J. R.; Hagler, A. T. An Ab Initio CFF93 All-Atom Force Field for Polycarbonates. *J. Am. Chem. Soc.* **1994**, *116*, 2978−2987.
(24) *Accelrys Software, Inc. Materials Studio Release Notes*, release 6.1; Accelrys Software, Inc.: San Diego, 2012.
(25) Rappé, A. K.; Goddard, W. A., III. Charge Equilibration for Molecular Dynamics Simulations. *J. Phys. Chem.* **1991**, *95*, 3358−3363.